Effects of black vinegar, Kurozu, on chromatin modifications and microRNA expression in the mouse liver

Yoshihiko Shibayama[1*], Akira Fujii[2], Yuki Fujimoto[2], Kensaku Hamada[2]

[1]Department of Drug Formulation, Faculty of Pharmaceutical Sciences, Health Sciences University of Hokkaido, 1757 Kanazawa, Tobetsu-cho, Ishikari-gun, Hokkaido 061-0293, Japan; [2]Sakamoto Kurozu, Inc., 21-15, Uenosono-chou, Kagoshima city, Kagoshima 890-0052, Japan.

*Corresponding author: Yoshihiko Shibayama, Ph.D., Department of Drug Formulation, Faculty of Pharmaceutical Sciences, Health Sciences University of Hokkaido, 1757 Kanazawa, Tobetsu-cho, Ishikari-gun, Hokkaido 061-0293, Japan.

ABSTRACT

Background: Kurozu is a traditional Japanese rice vinegar characterized by its brown color and that has been shown to improve hypertension, hypercholesterolemia, and carbohydrate metabolism. Kurozu has also been suggested to confer health benefits by altering gene expression; however, the molecular basis is not yet understood.

Objective: We previously reported that the intake of Kurozu increased the expression hepatic Sirt1 and microRNA (miR). These changes in gene expression may be attributed to histone modifications. Therefore, the current research explored the effects of supplementation with concentrated Kurozu (CK) on histone modifications in the liver.
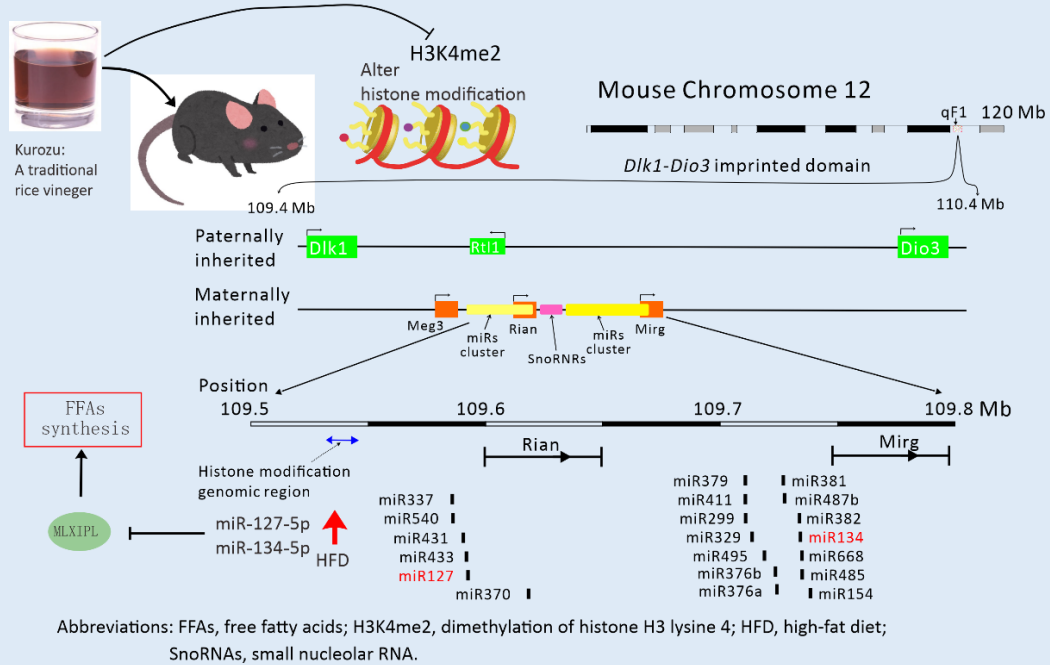
Methods: Over a period of 50 weeks, mice received a high-fat diet (HFD), HFD with CK, or a standard diet (SD). The study focused on the impact of CK on gene expression related to lipid metabolism in the liver.

Results: A microarray analysis revealed that HFD increased the expression of the miR cluster located on chromosome 12, while this change was suppressed by CK. The chromatin modification region upstream of the miR cluster was analyzed using a Chip assay. HFD significantly increased the levels of dimethylation of histone H3 lysine 4 (H3K4me2) and monoacetylation of histone H3 lysine 27 (H3K27ac). HFD also increased H3K4me2 levels, and this change was inhibited by HFD with CK. *MiR-127-5p* and *-134-5p*, which are present in the miR cluster, inhibited MLXIPL, a transcription factor involved in synthesizing fatty acids from carbohydrates. Further experiments with human colon cancer cells demonstrated that *miR-127-5p* and *-134-5p* significantly knocked down MLXIPL.

Conclusion: These results suggested that HFD affects miR expression levels by changing chromatin modification levels and that supplementation with CK suppressed HFD-induced increases in H3K4me2 levels. Furthermore, HFD upregulated the expression of *miR-127-5p* and *-134-5p*, which in turn suppressed MLXIPL.

Keywords: chromatin modification, genomic imprinting, high-fat diet, Kurozu, microRNA, MLXIPL

Black vinegar, Kurozu act on chromatin modification and microRNA expression

Abbreviations: FFAs, free fatty acids; H3K4me2, dimethylation of histone H3 lysine 4; HFD, high-fat diet; SnoRNAs, small nucleolar RNA.

INTRODUCTION

Vinegar is a common food flavoring reported to have health benefits. In particular, rice vinegar has been traditionally used in Japan and China, with Chinese grain vinegar being reported to be rich in amino acids and organic acids [1]. Kuroza, also known as black vinegar, is a rice vinegar also abundant in amino acids, which add umami to the taste [2]. It is manufactured in southern Japan using pottery and made from rice, Koji, and water. Koji is a culture of a specific species of mold on rice and barley, used in making Japanese sake, soy sauce, and miso. To produce Kuroza, alcohol fermentation and acetic acid fermentation must occur continuously in a ceramic pot, the product turning brown as it ages. The health benefits of Kurozu, including the attenuation of hypertension and hypercholesterolemia, have been reported since the 1980s [3]. As a result, Kurozu may be a potential functional food. To define it as such, it is necessary to

identify the bioactive compounds in the food that benefit health [5]. As aforementioned, Kuroza contains organic and amino acids, as well as acetic acid, which have been suggested to have important biological activities [2]. Recently, it was reported that components of Kurozu increased the levels of HSP1A, an important signaling molecule [6]. In addition, the acetic acid *bacteria A.* pasteurianus, utilized in the production of Kurozu, synthesizes *A. pasteurianus* lipolipod A, which is known to have a safe immune stimulating effect [7]. We also previously showed that concentrated Kurozu (CK) changed gene expression levels and upregulated the expression of Sirt1 and microRNA (miR) [4].

The nutritional status may affect the gene expression via post-translational modifications (PTM) in nucleosomes, which dynamically alter chromatin structure and reversibly modulate gene expression profiles. Histones are composed of four types of

proteins, including H3 and H4, and gene expression is activated or silenced by changes in the chromatin structure due to PTM, such as methylation and acetylation [8]. PTM modifications are reversible and affected by the dietary environment. Research has shown that a high-fat diet (HFD) impacts the methylation and acetylation of histone H3 lysine 4 (H3K4), H3K9, and H3K27, subsequently affecting the gene expression. The effects of histone modification on gene expression is conserved across different species, and H3K4me3 has been identified as a promoter marker and H3K27ac/H3K4me1 as an enhancer marker [9]. Gene imprinting plays a key role in transmitting the epigenome of gametes to the next generation of embryos. Imprinted genes that undergo genomic imprinting avoid reprogramming and maintain epigenomic information derived from the embryos' gametes. Histone methylation modulation controls genomic imprinting without DNA methylation. Found on chromosome 12 in mice and on chromosome 14 in humans, the *Dlk1-Dio3* locus is well-conserved among mammals [10, 11]. It is also involved in a wide range of developmental processes and pathological conditions in humans, such as genetic diseases and malignant tumors [12-14]. This locus contains the largest miR megacluster in the human genome, and it is a maternally imprinted gene cluster.

Also referred to as Carbohydrate-responsive element-binding protein (ChREBP), MLX Interacting Protein-like (MLXIPL) activates genes responsible for triglyceride synthesis in a carbohydrate concentration-dependent manner. MLXIPL also promotes lipid biosynthesis due to excessive carbohydrate intake, potentially exacerbating lifestyle-related diseases, such as fatty liver [15, 16]. In the current study, we examined the effects of HFD and CK on histone modifications to understand CK's impact on molecular functions in lipid and carbohydrate metabolism. In addition, we analyzed the effects of miR-127-5p and 134-5p, whose expression increased with HFD, on MLXIPL *in vitro*.

MATERIALS AND METHODS

Reagents: TOYOBO Co., Ltd. in Osaka, Japan supplied the THUNDERBIRD SYBR qPCR Mix, or real-time PCR master mix, and the ReverTra Ace, or reverse transcriptase. Synthetic PCR primers were procured from Fasmac Co., Ltd. in Atsugi, Japan, and their sequences are displayed in Table 1. Primer sequences were designed using PrimerBLAST. Rabbit monoclonal antibodies specific for histone (#5326, #8173, #9649, #9725, and #9751) were obtained from Cell Signaling in Danvers, USA. A mouse monoclonal antibody specific for CHREBP (2D9NB) was obtained from Novus Biologicals, LLC in CO, USA. FUJIFILM Wako Pure Chemical Corporation in Osaka, Japan provided the ScreenFect siRNA Transfection Reagent, ImmunoStar LD, RIPA buffer, GAPDH-targeting mouse monoclonal antibodies (specifically 5A12), anti-mouse IgG, peroxidase-conjugated rabbit polyclonal antibody, and all additional required reagents. The EpiQuik Chromatin Immunoprecipitation Kit was used for the Chip assay and procured from Epigentek Inc. in Farmingdale, USA. Finally, the Histone Acetyltransferase Activity Assay Kit (Colorimetric) was purchased from BioVision Incorporated in Milpitas, USA.

Animals: Male C57BL6J mice (7 weeks old, sourced from Hokudo, Sapporo, Japan) were kept in a controlled environment (maintained at 21 ± 2ºC with proper ventilation, under a 12-hour light/dark cycle). The 10-fold concentrated form of CK was acquired in a jar with a pH of 4.41 and obtained from Sakamoto Kurozu, Inc. in Kagoshima, Japan. The CK solution was composed of 3.2% lactic acid and 2.0% ash, with all acetic acid meticulously eliminated. Standard diet (CE-2) and high-fat diet feed (QuickFat) were procured from CLEA Japan, Inc. in Tokyo, Japan. CE-2 is comprised of 4.8% fat derived from soybeans and wheat germ, while QuickFat has 13.9% fat sourced from cattle suet and wheat germ. In QuickFat, black vinegar forage contains 0.6% (V/W) concentrated black vinegar. Throughout the 50-week chronic treatment period, the animals were provided ad libitum access to forage and water. The standard diet group received CE-

2, the high-fat diet group (HFD) received QuickFat, and the CK group received QuickFat containing CK. Following blood collection, mice were humanely sacrificed by exsanguination. Target tissues were swiftly excised and preserved at –30°C for subsequent Western blot analysis. Tissues designated for RNA analysis were preserved in RNAlater solution at –30°C to ensure the stability and integrity of cellular RNA until RT-PCR analysis. Serum samples obtained from each mouse were stored at 4°C until analyzed. The current study was approved (approval number, 20-047) in accordance with the guidelines of the Health Science University of Hokkaido regarding the ethical use and treatment of experimental animals.

Cell culture and transfection assays: The human adenocarcinoma cell lines, COLO201 (JCRB0226) and WiDr (JCRB0224) were procured from the Japanese Collection of Research Bioresources Cell Bank in Osaka, Japan. The JCRB Bank conducted testing on and authentication of these cell lines. COLO201 cells were cultured in Dulbecco's Modified Eagle Medium (DMEM) enriched with 2 mM glutamine, 10% fetal bovine serum, and 100 units/mL of penicillin, maintained at 37°C in a 5% CO_2 humidified atmosphere. Synthetic *MLXIPL* siRNA (MISSION predesign) was acquired from Merck KGaA (EHU094041, Darmstadt, Germany). Synthetic miR (AcuTarget predesignmiRNA mimics) were purchased from Bioneer in Daejeon, Republic of Korea. Transfection of synthetic *MLXIPL* or negative control siRNA (AllStars Negative Control siRNA, QIAGEN, Valencia, CA, USA) was conducted using the ScreenFect siRNA Transfection Reagent as per the protocol of the manufacturer.

Bioinformatics analysis: Bioinformatics tools were used to predict the minimum free energies (MFE) and binding modes of the complementary binding between the 3' UTR region of mRNA and miR. These predications were made using RNAhybrid, accessible at bibiserv.techfak.uni-bielefeld.de/rnahybrid/. Sequence information for the 3' UTR region of mRNA

and miR was collected from microrna.org.

Assays and microarray analysis: Protein concentrations were measured using the DC protein assay. Optical densities in the Western blotting analysis were measured with ImageJ, a publicly available software created by the US National Institute of Health and accessible at rsb.info.nih.gov/ij/download.html. Aging-related hormone concentrations were assessed according to the instructions of the manufacturer. Messenger RNA for the microarray analysis was purified using the RNeasy Plus Mini kit, followed by microarray analysis with the GeneChip™ miRNA 4.0 Array by Filgen Inc. in Nagoya, Japan. The Chip assay was performed according to the instruction manual using monoclonal antibodies specific for histone with a 1,000-fold dilution. PCR primers recognizing the histone modification region [17] (position: 109,528,401 - 109,543,470) on mouse chromosome 12, 12qF1 and the histone modification region (position: 65,820,042 - 66,654,578) located on mouse chromosome X, 12qA7.1 upstream of the miR cluster were created. Primer sets were used for the Chip assay, and the primer sequences are displayed in Table 1.

Real-time quantitative RT-PCR analysis: Total RNA was extracted from target tissues using ISOGEN II Reagent, following the manufacturer's protocol. The miR expression levels were measured using the miScript Primer Assay and miScript Reverse Transcription kit (QIAGEN, Valencia, CA, USA). Single-stranded cDNA was synthesized using ReverTra Ace following the manufacturer's instructions. The relative expression levels of target genes were assessed by the comparative quantification cycle threshold (Cq) method, with Cq values being computed using the 2nd derivative maximum method. GAPDH served as the reference gene for mRNA analysis. The cycle number difference (ΔC_q = reference genes – target genes) was computed for each replicate, and the mean of ΔCq from duplicates, $\mu(\Delta Cq) = (\Sigma\Delta Cq)/2$, was expressed as $2^{\mu(\Delta Cq)}$ to determine the relative target gene expression values.

Table 1. Primer sequences.

	Forward (5' > 3')	Reverse (5' > 3')	Product length
Beta2M	TGGGAAGTCTAGGGAGGAGC	CATCCCATTCTGCACACCCT	136
Rian	TGCATAGGCTCCTTTCAGCC	ACAGATCTTGTGCCACCCTG	115
Mirg	AGCTTCTGGGGTGAACATGG	ACCCGCCAGCTTCTGAATAC	144
Chr12-1	AGGGAGAAGATTGCAAGCCC	AAACCATGCTGAGCCTACCC	178
Chr12-2	AGTGAGCTTGACCTGGAAGC	CAGCCCACAGAGGCCAATAA	236
Chr12-4	GGCCTGGCAAAAAGGGAATG	TAGTCACCGGCCTATCCACA	130
Chr12-6	TGGACCTCAGGGACCAAGAA	GCTGGAGCTTGGCACTAGAA	119
Chr12-8	TCGAGAACGGCATAGGCTTC	GCAGCAGCCTGGAAAAGAAC	265
ChrX-1	TTTTAGCATGTAGGGCGGGC	CACAAAGTTTGGCAGTCAACCA	147
ChrX-2	GCCCAGTTTTATGAAGGCACT	TGTCAAGTTGGCACACACAC	57
ChrX-5	CCATCGTGCTGCATGTTTTCA	TCAGAGAATGCCTATTCAGCACT	108
GAPDH	AACAGCCTCAAGATCATCAGC	GGATGATGTTCTGGAGAGCC	200
MLXIPL	CCGGCGTATCACACACATCT	AAGGACTCAAACAGAGGCCG	399

Chr 12-1 -8: Primers were designed to recognize positions 109,543,000 to 109,549,000 of mouse chromosome 12. ChrX-1 -5: Primers were designed to recognize positions 65,820,042 to 66,654,578 of mouse chromosome X. The gene region undergoes chromatin modifications [17].

Electrophoresis and Western blotting: The entire cell population was lysed in RIPA buffer supplemented with a protease inhibitor. Protein concentrations were quantified using the Protein Assay Kit from Nacalai Tesque, Kyoto, Japan. Whole cell homogenates containing 5 µg of GAPDH and 20 µg of MLXIPL were separated by SDS polyacrylamide gels, followed by transfer of proteins onto nitrocellulose membranes. The membranes were blocked with Blocking One from Nacalai Tesque, Inc., Kyoto for 1 hour at room temperature. They were then incubated with primary antibodies at dilutions of 500-fold for MLXIPL and 10,000-fold for GAPDH. After three washes with Tris-buffered saline with Tween®20 (TBS-T), the membranes were further cultured with a secondary antibody conjugated with peroxidase at a dilution of 20,000-fold. Following one 15-minute rinse and four 5-minute rinses with TBS-T, protein bands were detected using the ImmunoStar LD Western blotting detection system.

RESULTS

CK increased miR expression levels in the liver and serum: The effects of CK on gene expression levels were evaluated. Both mRNA and miR expression levels were assessed using microarray analyses. HFD significantly affected mRNA and miR expression levels in the liver (Table 2). The microarray analysis suggested that miR expression levels were significantly affected by HFD. The miR showing changes in their expression levels formed gene clusters (Figure 2). A cluster of 51 miR on mouse chromosome 12 qF1 was observed in a small genomic region of 300 kb (Figure 2A). Increases in expression levels were suppressed by CK. Additionally, the expression of miR located in mouse chromosome X qA7.1 in a region of approximately 70 kb was significantly suppressed by HFD (Table 2, Figures 1 and 3). The expression levels of miR were also assessed using RT-PCR. Consistent with the microarray method results, expression levels in the liver and plasma were increased by HFD (Tables 3 and 4). The expression of miR-127-5p in plasma was markedly increased (Table 4). The expression level of *Mirg* was significantly increased by HFD (Table 3).

HFD affected hepatic histone modifications: We investigated changes in chromatin modifications concerning the chronic ingestion of HFD. Histone acetyltransferase (HAT) activity in the liver was significantly higher in the HFD group compared to the SD group and was slightly increased in the CK group (Figure 2B). Levels of monoacetylation of histone H3 lysine 27 (H3K27ac) and dimethylation of histone H3 lysine 4 (H3K4me2) levels were also significantly higher in the HFD group compared to the SD group (Figures 2C

and D). H3K27ac levels were significantly increased in the CK group. H3K4me2 levels increased in the HFD group, but not in the CK group. The trimethylation of histone H3 lysine 4 (H3K4me3) increased in the HFD group, while levels in the CK and SD groups were similar. H3K9ac and H3K4me levels were slightly increased by HFD (data not shown). H3K4Mm and H3K4me3 levels were significantly increased by HFD upstream of the miR cluster located on chromosome X. H3K4me levels were higher in the HFD group than in the CK group. No significant changes were observed in the levels of H3K9ac, H3K27ac, or H3K4me2 upstream of the miR cluster among the three groups.

Table 2. Microarray-based evaluation of miRs expression in the liver 50 weeks of feeding.

	SD	HFD	HFD with CK
mmu-miR-127-5p	1.20 ± 0.20	34.28 ± 1.56	1.13 ± 0.09
mmu-miR-134-5p	5.03 ± 3.41	278.65 ± 169.95	2.15 ± 0.62
mmu-miR-337-5p	1.20 ± 0.05	4.53 ± 2.35	1.18 ± 0.09
mmu-miR-370-3p	1.62 ± 0.23	22.04 ± 15.98	1.86 ± 0.17
mmu-miR-376b-3p	1.78 ± 0.09	425.99 ± 273.39	1.56 ± 0.21
mmu-miR-379-5p	18.24 ± 13.74	1743.28 ± 1176.54	2.75 ± 0.34
mmu-miR-409-3p	1.53 ± 0.17	75.33 ± 51.13	1.25 ± 0.27
mmu-miR-485-5p	1.33 ± 0.15	88.22 ± 61.41	1.31 ± 0.03
mmu-miR-543-3p	1.25 ± 0.18	67.05 ± 43.21	1.32 ± 0.04

Values provided indicate the raw data (mean ± standard error, n = 3) of expression levels measured in the liver. The results were obtained using the microarray analysis, GeneChip™ miRNA 4.0. The miRs, whose expression was increased by HFD feeding compared with SD received group, were shown. No significant differences were observed among the three groups. Statistical analyses were carried out via the Tukey-Kramer test.
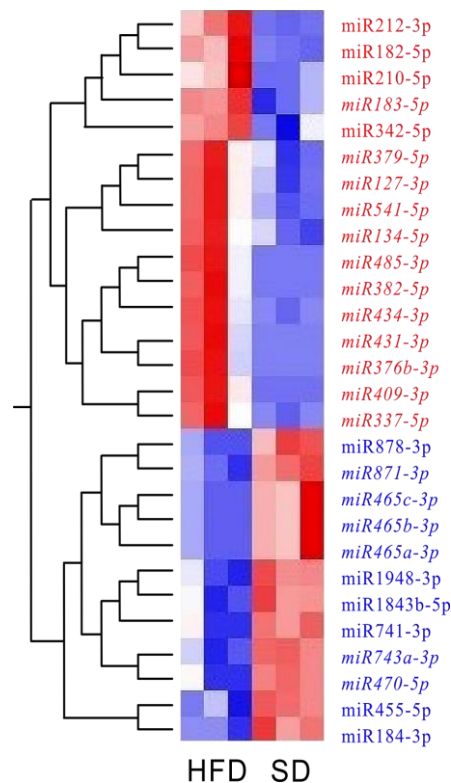

Figure 1. Heat map of miR with expression levels affected by HFD. Red indicates miR with increases in expression by HFD, while blue indicates miR with decreases in expression by HFD. MiR, with an expression ratio of 2 times or more and p values <0.05 (n=3), are shown. Significant differences were observed between SD and HFD groups, but not between SD and CK groups, as indicated in italics. The analysis was performed using the Qlucore Omics Explorer.

Table 3. Relative expression levels of miR and mRNA in the liver after 50 weeks of feeding.

	SD	HFD	HFD with CK
mmu-miR-127-5p	1.00 ± 0.08	7.48 ± 1.36**	5.65 ± 0.89*
mmu-miR-134-5p	1.00 ± 0.07	4.14 ± 0.51**	3.14 ± 1.07
mmu-miR-337-5p	1.00 ± 0.08	2.68 ± 0.32*	2.92 ± 0.96*
mmu-miR-370-3p	1.00 ± 0.07	3.73 ± 0.52**	2.35 ± 0.33
mmu-miR-376b-3p	1.00 ± 0.07	3.60 ± 0.70*	3.70 ± 0.59*
mmu-miR-379-5p	1.00 ± 0.07	3.26 ± 0.49*	3.26 ± 0.71*
mmu-miR-409-3p	1.00 ± 0.04	3.29 ± 0.75**	2.36 ± 0.34
mmu-miR-485-5p	1.00 ± 0.07	3.26 ± 0.51*	3.63 ± 0.58**
mmu-miR-543-3p	1.00 ± 0.09	2.79 ± 0.40*	2.70 ± 0.44**
Rian	1.01 ± 0.05	0.86 ± 0.30	1.41 ± 0.29
Mirg	1.02 ± 0.06	1.71 ± 0.12**	1.85 ± 0.18**

Values provided indicate the relative ratio (mean ± standard error, n = 4) of expression levels measured in the liver. Statistical analyses were carried out via the Tukey-Kramer test, with[**] $P < 0.01$ and [*] $P < 0.05$ highlighting significant differences compared to expression levels observed in the SD group.

Table 4. Relative expression levels of miR in serum after 50 weeks of feeding.

	SD	HFD	HFD with CK
mmu-miR-127-5p	1.00 ± 0.10	46.60 ± 6.91**	69.55 ± 11.52**
mmu-miR-134-5p	1.00 ± 0.12	0.94 ± 0.17	1.57 ± 0.34
mmu-miR-337-5p	1.00 ± 0.07	8.14 ± 2.98	3.60 ± 0.58
mmu-miR-370-3p	1.00 ± 0.06	10.90 ± 4.46*	11.81 ± 3.63*
mmu-miR-376b-3p	1.00 ± 0.06	3.74 ± 0.88**	3.31 ± 0.42**
mmu-miR-379-5p	1.00 ± 0.19	3.59 ± 0.53*	5.34 ± 0.80**
mmu-miR-409-3p	1.00 ± 0.07	2.07 ± 0.21*	3.31 ± 0.41**
mmu-miR-485-5p	1.00 ± 0.09	3.27 ± 0.66**	4.17 ± 0.56**
mmu-miR-543-3p	1.00 ± 0.09	2.73 ± 0.55*	2.96 ± 0.53*

Values provided indicate the relative ratio (mean ± standard error, n = 4) of expression levels measured in the liver. Statistical analyses were carried out via the Tukey-Kramer test, with [**] $P < 0.01$ and [*] $P < 0.05$ highlighting significant differences compared to expression levels observed in the SD group.

MiR-127-5p and -134-5p down-regulated MLXIPL: miR-127-5p mimic, miR-134-5p mimic, or *MLXIPL* siRNA were introduced into the human carcinoma cell lines WiDr and COLO201. Transfection with miR-127-5p or -134-5p mimic resulted in a significant decrease in *MLXIPL* mRNA expression levels, while positive control siRNA down-regulated *MLXIPL* expression (Table 5). Furthermore, transfection with miR mimics also led to a significant down-regulation of *MLXIPL* expression (Figure 4A, Table 5). Subsequently, a bioinformatics analysis was conducted to predict the complementary miR sequences for *MLXIPL*. RNAhybrid, accessible via bibiserv.techfak.uni-bielefeld.de/rnahybrid/, serves as an extensive repository for miR target predictions, encompassing extreme value statistics on length-normalized MFE [18, 19]. According to RNAhybrid's estimation, has-miR-127-5p and -134-5p form complexes with *MLXIP*L mRNA. The predicted alignment configurations and associated MFE are provided in Figure 4B.
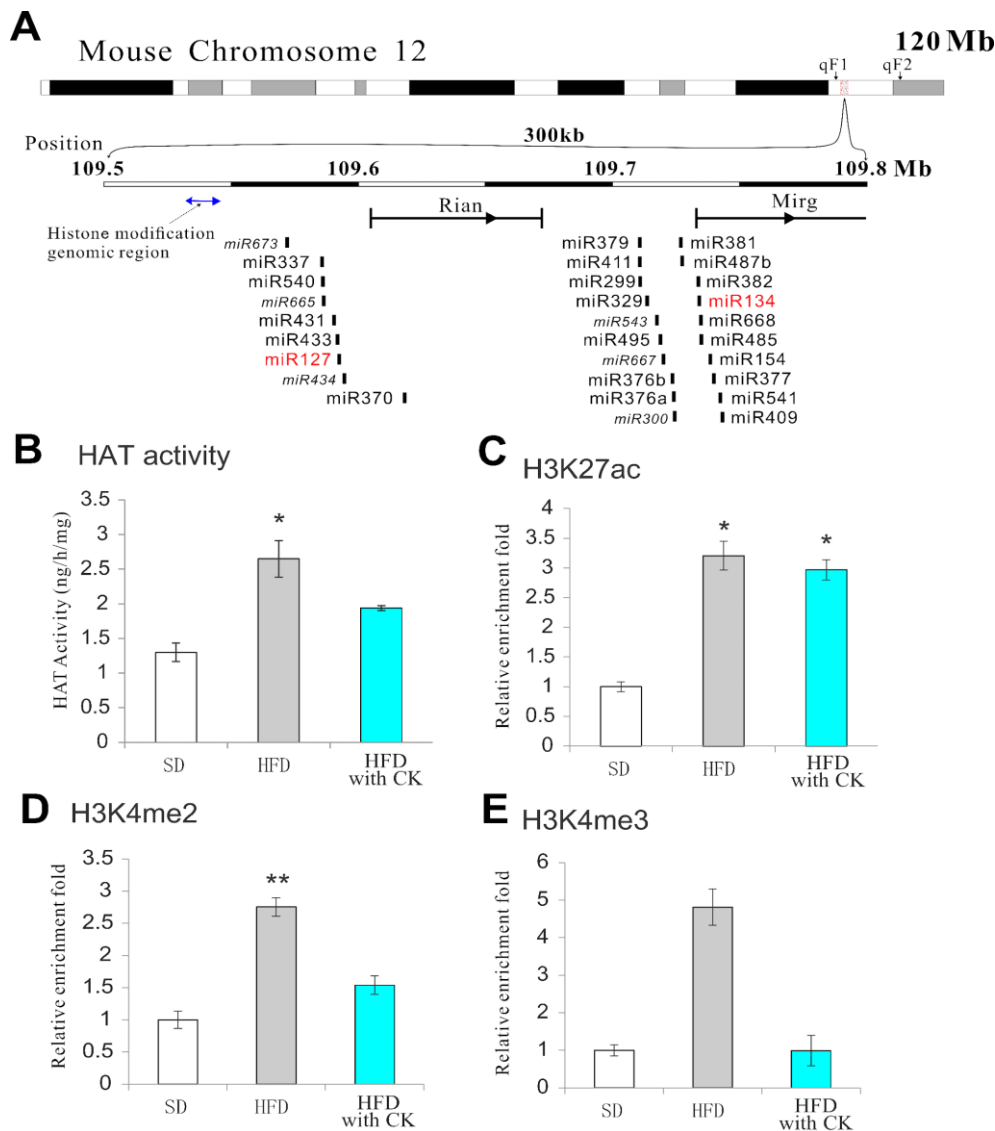
Figure 2. Schematic diagram of the microRNA gene map on mouse chromosome 12. SD: standard diet; HFD: high-fat diet; HFD with CK: HFD with concentrated Kurozu. (A) The ingestion of a high-fat diet (HFD) significantly increased the expression of microRNAs on chromosome 12. microRNAs with increased expression formed a gene cluster near 12qF1 (Location: 109.55-109.80 M bases) of chromosome 12, which consisted of approximately 120 M bases. Rian and Mirg were also present in the genetic region. A histone modification region was detected upstream of the gene cluster, and PCR primers that recognize the region were created. These PCR primers were used in the CHIP assay. Primer sequences are shown in Table 1. (B) Histone acetyltransferase (HAT) activity in the liver, measured using a kit and expressed in its calibration curve units. Values represent the mean ± standard error. HFD significantly increased HAT activity, while a significant difference was not observed in the CK group. (C) Relative enrichment of the histone modification of H3K27ac in the genomic region (shown as a fold change). HFD significantly enhanced the histone modification of H3K27ac. HFD with CK also significantly enhanced the histone modification of H3K27ac. (D) Relative enrichment of the histone modification of H3K4me2 in the genomic region (shown as a fold change). HFD significantly enhanced the histone modification of H3K4me. HFD with CK did not significantly enhance the histone modification of H3K4Me2. (F) Relative enrichment of the histone modification of H3K4me3 in the genomic region (shown as a fold change). HFD enhanced the histone modification of H3K4me3. A significant difference was not observed. Values provided indicate the relative ratio (mean ± SE) of expression levels measured in the liver. Statistical analyses were carried out via the Tukey-Kramer test, with ** $P < 0.01$ and * $P < 0.05$ highlighting significant differences compared to expression levels in the SD group.
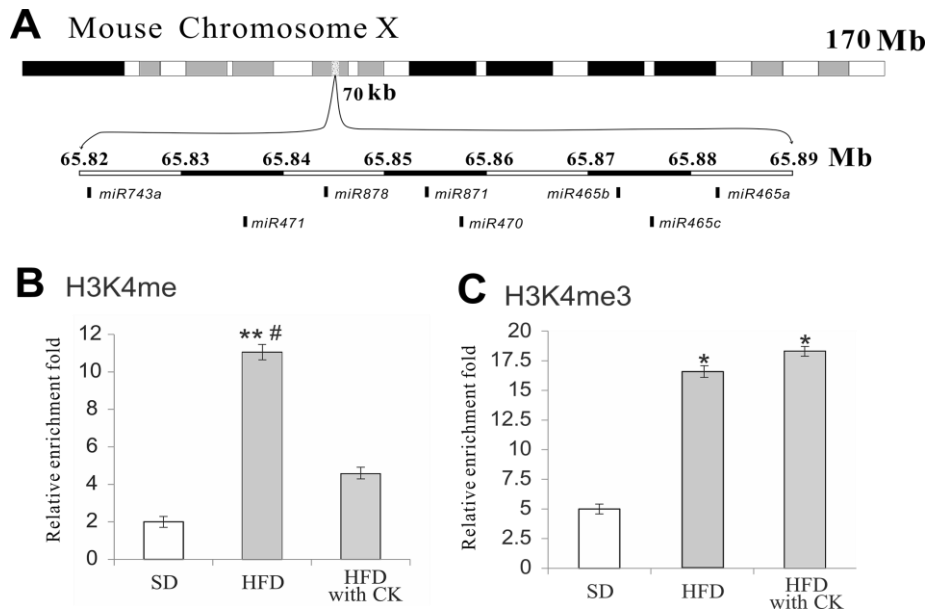
Figure 3. MiR clusters with expression levels that were decreased by HFD. (A) The expression of miR located in mouse chromosome X qA7.1 in a region of approximately 70 kb was significantly suppressed by HFD. (B) Relative enrichment of the histone modification of H3K4Me in the genomic region. HFD significantly enhanced the histone modification of H3K4me. A significant difference was observed between the HFD and HFD with CK groups. Values represent the relative ratio (mean ± SE) of expression levels in the liver. (C) Relative enrichment of the histone modification of H3K4me3 in the genomic region (shown as a fold change). HFD and HFD with CK significantly enhanced the histone modification of H3K4me3. Statistical analyses were carried out via the Tukey-Kramer test, with ** $P < 0.01$ and * $P < 0.05$ highlighting significant differences compared to expression levels in the SD group. # $P < 0.05$ highlighted significant differences from expression levels in the HFD with CK group.
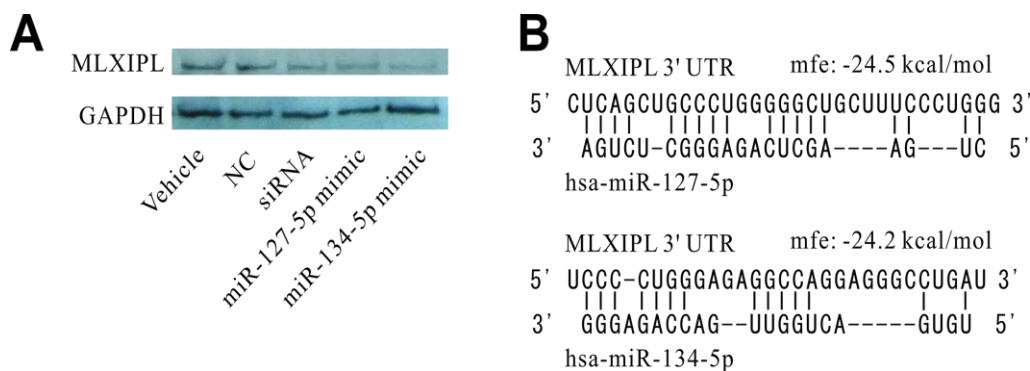

Figure 4. (A) Standard Western blot images of MLXIPL and GAPDH. miR-127-5p and miR-134-5p mimics significantly suppressed the expression of MLXIPL in COLO201 cells. A positive control, MLXIPL siRNA, also significantly suppressed expression. SDS polyacrylamide gels were used to separate whole cell homogenates (MLXIPL: 20 µg; GAPDH: 5 µg). MLXIPL and GAPDH proteins were observed as 98- and 36-kDa bands, correspondingly. Relative expression values are shown in Table 4. (B) A bioinformatics analysis estimated that has-miR-127-5p and has-miR-134-5p complementarily bound to the 3' UTR of *MLXIPL* mRNA. RNAhybrid, accessible via http://bibiserv.techfak.uni-bielefeld.de/rnahybrid/, serves as an extensive repository for miR target predictions encompassing extreme value statistics on length-normalized MFE. According to RNAhybrid's estimation, has-miR-127-5p and has-miR-134-5p are bound (positions: 22 and 433) to the 3' UTR of *MLXIPL* in the optimized form. The predicted alignment configurations and associated MFE are provided.

Table 5. MLXIPL knockdown in adenocarcinoma cells by siRNA or miR transfection.

mRNA				
	NC	siRNA	hsa-miR-127-5p	hsa-miR-134-5p
WiDr	1.00 ± 0.13	0.21 ± 0.08[**]	0.24 ± 0.10[**]	0.06 ± 0.02[**]
COLO201	1.00 ± 0.13	0.14 ± 0.05[**]	0.11 ± 0.04[**]	0.22 ± 0.09[**]
Protein				
	NC	siRNA	hsa-miR-127-5p	hsa-miR-134-5p
WiDr	1.00 ± 0.02	0.54 ± 0.05[**]	0.55 ± 0.07[**]	0.52 ± 0.05[**]
COLO201	1.00 ± 0.05	0.48 ± 0.04[***]	0.59 ± 0.06[***]	0.60 ± 0.04[**]

Mimics of miR-127-5p, -129-5p, and -134-5p transfection inhibited *MLXIPL* expression. Values provided indicate the relative ratio of *MLXIPL* expression per *GAPDH* (mean ± SEM) compared to the control from independent experiments, n = 4. Negative control RNA was used to transfect the negative control group (NC). Statistical analyses were carried out via the Tukey-Kramer test, with significance levels of ***$P < 0.001$, **$P < 0.01$, *$P < 0.05$.

DISCUSSION

Nutritional status affects gene expression through epigenetic mechanisms [20]. We previously reported that HFD and CK changed hepatic gene expression levels in mice. In the present study, we examined the effects of HFD and CK on miR expression in the mouse liver. Changes in hepatic miR expression levels were comprehensively observed using a microarray method. A previous study demonstrated that HFD did not induce inflammation in the liver after 40 weeks of feeding, but hyperplasia of the liver developed after one year of feeding [21]. The present results also showed that fatty liver developed after 20 weeks of feeding, while hyperplasia occurred after 60 weeks of feeding [4]. Based on previous findings, the breeding period was set at 50 weeks in the current study.

The microarray analysis identified 43 miR with expression levels that changed by a Log2 value of 3 or more (ratio of 8 times or more, Table 2). Forty-one of the 43 miR genes were clustered in specific regions on 12 chromosomes (Figure 2). Their miR expression levels were also evaluated by RT-PCR (Tables 3, 4). Similarities in the effects of HFD on gene expression were observed in both the microarray analysis and RT-PCR results. The expression of *Mirg*, an ncRNA located in the gene region of the miR cluster, was significantly upregulated by HFD (Table 3). Among miR with increased expression levels in the HFD group, the expression levels of hepatic *miR-134-5p*, *-370-5p*, and *-490-3p* did not significantly

differ from those in the HFD with CK and SD groups. These results suggest that CK affected HFD-induced changes in miR expression. However, since the number of samples examined was small, additional research is needed to clarify the effects of CK.

Previous studies reported that HFD increased the expression of miR-124 [22], -222 [23], -367 [24], and -665-3p [25]. Yu et al. (2022) showed that HFD for 24 weeks increased hepatic mmu-miR-367-3p expression levels in mice. The present study also illustrated that miR-367-3p expression levels increased after 50 weeks of HFD [24]. Additionally, Zhang et al. (2019) found that HFD for four weeks increased aortic *rno-miR-134-5p* in rats [26]. The current results demonstrated that HFD significantly increased the expression of hepatic miR-134-5p, whereas HFD with CK did not. Significant differences were found in the serum levels of *mmu-miR-134-5*p among the SD, HFD, and HFD with CK groups (Table 4), but not between the SD and HFD with CK groups. Since CK may affect mmu-miR-134-5p expression, further studies are required to clarify the effects of CK supplementation. *mmu-miR-127-3p* expression levels were increased by HFD. Auler et al. (2021) reported that the expression level of *mmu-miR-127-3p* was increased in a skin wound model [27]. Furthermore, *mmu-miR-127-3p* expression levels were elevated by inflammation in a model simulating non-alcoholic fatty liver disease. The current study revealed that HFD significantly increased the expression level of

miR-127-5p in serum. Therefore, serum *miR-127-5p* has potential as a biomarker for fatty liver [28].

The miR cluster with increased expression levels due to HFD was present in the *Dlk1-Dio3* locus (Position: 109.4 – 110.4 Mb) on mouse chromosome 12. HFD has been shown to affect the expression of the imprinted, paternally inherited genes Igf2 and Peg3; however, the effects of HFD on epigenetic modifications in the *Dlk1-Dio3* locus remain unknown. A recent study reported that diet deficient in vitamin B9 and B12 increased miR-134-5p and miR-369-5p levels at the *Dlk1-Dio3* locus and H3K9me3 levels in the cerebellum of male rats [29]. The methylation of histone modification regions activates gene expression, and cells utilize the methylation of H3K4 as a mechanism to tag promoters and enhancers. Active promoters are tagged with H3K4me3, while enhancers are tagged with H3K4me and H3K4me2 [30]. It remains unclear whether HFD affects the histone modification region upstream of miR clusters. It has been reported that miRNA expression in the *DLK1-DIO3* imprinted region is involved in pathogenic mechanism. Dysregulation of select *DLK1-DIO3* miRNAs has been identified in various biological samples from human lupus patients [31]. Jin et al. (2022) found that miR expression in *Dlk1-Dio3* is elevated in multiple sclerosis patients and that miRNA in the *DLK1-DIO3* imprinted region may promote the progression of hepatocellular carcinoma [32]. We also previously reported that CK

supplementation suppresses the development of hepatocellular carcinoma [33]. It is thought that the changes in histone modification and miR expression observed in this report following CK supplementation may affect the proliferation of hepatocellular carcinoma cells. The current study is the first to show that HFD upregulates the expression of the miR cluster in the *Dlk1-Dio3* locus. Although CK significantly decreased the level of H3K4me2 more than HFD, further investigation is necessary to elucidate the mechanisms by which HFD and CK affect cellular functions through changes in miR expression.

To investigate the functions of miR-127-5p and -134-5p, whose expression was increased by HFD, we examined their interaction with MLXIPL, an important transcription factor for lipid and carbohydrate metabolism. Bioinformatics analysis suggested that MiR-127-5p and -134-5p complementarily bind to MLXIPL. Experiments using human colon cancer cells demonstrated significant inhibition of mRNA and protein expression. These results indicated that miR-127-5p and -134-5p suppress MLXIPL. An excessive intake of lipids and carbohydrates may suppress fatty acid synthesis by inhibiting MLXIPL (Figure 5). The present study suggested that HFD increases H3K4me2 and H3K27ac levels and that CK changes miR expression patterns by suppressing the HFD-induced increase in H3K4me2 levels.
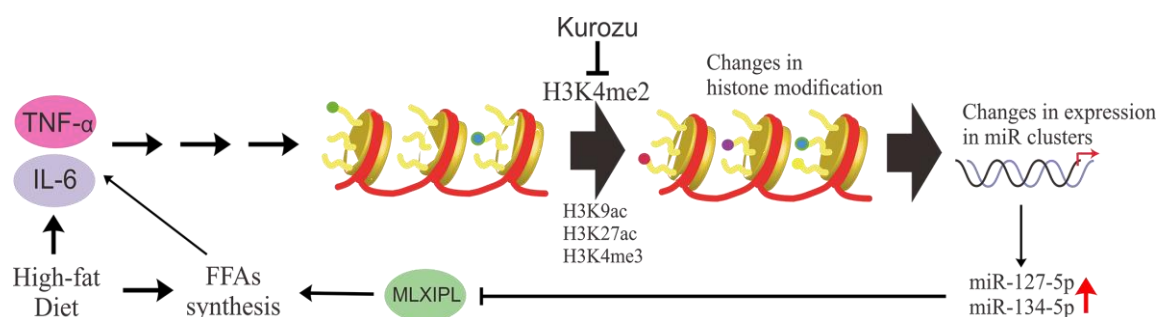

Figure 5. A possible mechanism suppressing HFD-induced changes in histone modifications. The ingestion of HFD increased the production of adipocytokines from adipose tissue, which enhanced the production of inflammatory cytokines, such as TNF-α and IL-6. HFD also increased free fatty acids, which, in turn, increased inflammatory cytokines. MLXIPL is an enzyme that catalyzes fatty acid synthesis. *MiR-127-5p* and *miR-134-5p* inhibit MLXIPL protein synthesis and may suppress increases in inflammatory cytokines. Abbreviations: FFAs, free fatty acids; IL-6, interleukin-6; TNF-α, tumor necrosis factor-alpha.

CONCLUSION

1. HFD alters gene expression levels in the mouse liver. Genes with affected expression levels were concentrated in specific genomic regions, with increased expression observed in the *Dlk1-Dio3* imprinted domain on chromosome 12 and with decreased expression observed in a region on the X chromosome.

2. Levels of H3K4me2, H3K4me3, and H3K27ac modifications were increased in the *Dlk1-Dio3* imprinted domain. Kurozu supplementation significantly attenuated the increase in H3K4me2 modification levels associated with HFD intake.

3. The HFD increases expression levels of *miR-127-5p* and *-134-5p* within the *Dlk1-Dio3* imprinted domain. Experiments using human colon cancer cells revealed that these *miRs* collectively suppress MLXIPL, an important transcription factor for lipid metabolism and synthesis. It was predicted that increased levels of *miR-127-5p* and *-134-5p* due to HFD would suppress MLXIPL, thereby reducing free fatty acid synthesis.

4. HFD increases the expression of *miRs* in the *Dlk1-Dio3* imprinted domain, but supplementation with Kurozu suppresses this increase. It has been reported that Kurozu improves lipid and carbohydrate metabolism. The results of this study suggest that these functional changes may be related to its effects on chromatin modification levels.

List of Abbreviations: CK, concentrated Kurozu; H3K4, histone H3 lysine 4; H3K9, histone H3 lysine 9; HAT, Histone acetyltransferase; HFD, high-fat diet; miR: microRNA; MFE: minimum free energies; MLXIPL, MLX Interacting protein like; PTM, post-translational modification.

Competing Interests: Fujii, Fujimoto, and Hamada are employees of Sakamoto Kurozu Co., Ltd. Shibayama has no conflicts of interest to disclose.

Authors' Contributions: Kurozu brewing: A.F., Y.F. and K.H. Animal and *in vitro* experiments: Y.S. Data analysis: Y.S. Writing-original draft: Y.S. Writing-review and editing: Y.S., A.F., Y.F., and K.H.

REFERENCES

1. Li Z, Zhao C, Dong L, Huan Y, Yoshimoto M, Zhu Y, Tada I, et al: Comprehensive metabolomic comparison of five cereal vinegars using non-targeted and chemical isotope labeling LC-MS analysis. Metabolites 2022, 12(5):427.
   DOI: https://doi.org/10.3390/metabo12050427

2. Yanagihara N, Maeda M, Yoshikawa J, Akuzawa, S, Fujii A, Nagano M, Koizumi Y, et al: Flavor assessment of a lactic fermented vinegar described in Japanese books from the Edo period (1603–1867). Heliyon 2024, 10(11):E32344.
   DOI: https://doi.org/10.1016/j.heliyon.2024.e32344

3. Shibayama Y, Kanouchi H, Fujii A, Nagano M: A review of Kurozu, amber rice vinegar made in pottery jars. Funct Foods Health Dis 2020, 10:254-264.
   DOI: https://doi.org/10.31989/ffhd.v10i6.713

4. Shibayama Y, Nagano M, Fujii A, Hashiguchi K, Morita S, Kubo Y, Nakagawa T: Effect of concentrated Kurozu, a traditional Japanese vinegar, on expression of hepatic miR-34a, -149-3p, and -181a-5p in high-fat diet-fed mice. Funct Foods Health Dis 2020, 10:1-17.
   DOI: https://doi.org/10.31989/ffhd.v10i1.668

5. Martirosyan D, Lampert T, Lee M: A comprehensive review on the role of food bioactive compounds in functional food science. Funct Foods Sci 2022, 3(2):64-78.
   DOI: https://doi.org/10.31989/ffs.v2i3.906

6. Nonaka M, Kanouchi H, Torii S, Nagano H, Kondo S, Fujii A, Nagano M, et al: Lactic acid induces HSPA1A expression through ERK1/2 activation. Biosci Biotechnol Biochem 2023. 87(2):191-196.
   DOI: https://doi.org/10.1093/bbb/zbac192

7. Yamaura H, Shimoyama A, Hosomi K, Kabayama K, Kunisawa J, Fukase K: Chemical synthesis of acetobacter pasteurianus lipid A with a unique tetrasaccharide backbone and evaluation of its immunological functions. Angewandte Chemie Int Ed 2024, 63(2410):e202402922.
   DOI: https://onlinelibrary.wiley.com/doi/10.1002/ange.202402922

8. Molina-Serrano D, Kyriakou D, Kirmizis A: Histone modifications as an intersection between diet and longevity. Front Genet 2019, 10:192.
   DOI: https://doi.org/10.3389/fgene.2019.00192

9. Ho JW, Jung YL, Liu T, Alver BH, Lee S, Ikegami K, Sohn KA, et al.: Comparative analysis of metazoan chromatin organization. Nature 2014, 512:449-452.
   DOI: https://doi.org/10.1038/nature13415

10. da Rocha ST, Edwards CA, Ito M, Ogata T, Ferguson-Smith AC: Genomic imprinting at the mammalian Dlk1-Dio3 domain. Trends Genetics 2008, 24:306-316. DOI: https://doi.org/10.1016/j.tig.2008.03.011

11. Weinberg-Shukron A, Youngson NA, Ferguson-Smith AC, Edwards CA: Epigenetic control and genomic imprinting dynamics of the Dlk1-Dio3 domain. Front Cell Dev Biol 2023, 11:1328806. DOI: https://doi.org/10.3389/fcell.2023.1328806

12. Benetatos L, Hatzimichael E, Londin E, Vartholomatos G, Loher P, Rigoutsos I, Briasoulis E: The microRNAs within the DLK1-DIO3 genomic region: involvement in disease pathogenesis. Cell Mol Life Sci 2013, 70:795-814. DOI: https://doi.org/10.1007/s00018-012-1080-8

13. Ogata T, Kagami M: Kagami–Ogata syndrome: a clinically recognizable upd(14)pat and related disorder affecting the chromosome 14q32.2 imprinted region. J Hum Genet 2016, 61:87-94. DOI: https://doi.org/0.1038/jhg.2015.113

14. Li J, Shen H, Xie H, Ying Y, Jin K, Yan H, Wang S, et al: Dysregulation of ncRNAs located at the DLK1-DIO3 imprinted domain: Involvement in urological cancers. Cancer Manag Res 2019, 11:777-787. DOI: https://doi.org/10.2147/CMAR.S190764

15. Iizuka K: The transcription factor carbohydrate-response element-binding protein (ChREBP): A possible link between metabolic disease and cancer. Biochim Biophys Acta Mol Basis Dis 2017, 1863:474-485. DOI: https://doi.org/10.1016/j.bbadis.2016.11.029

16. Iizuka K, Takao K, Yabe D: ChREBP-Mediated Regulation of Lipid Metabolism: Involvement of the gut microbiota, liver, and adipose tissue. Front Endocrinol (Lausanne). 2020, 11:587189. DOI: https://doi.org/10.3389/fendo.2020.587189

17. Gorkin DU, Barozzi I, Zhao Y, Zhang Y, Huang H, Lee AY, Li B, et al: An atlas of dynamic chromatin landscapes in mouse fetal development. Nature 2020, 583:744-751. DOI: https://doi.org/10.1038/s41586-020-2093-3

18. Krüger J, Rehmsmeier M: RNAhybrid: MicroRNA target prediction easy, fast and flexible. Nucleic Acids Res 2006, 34:W451-454. DOI: https://doi.org/0.1093/nar/gkl243

19. Rehmsmeier M, Steffen P, Hochsmann M, Giegerich R: Fast and effective prediction of microRNA/target duplexes. RNA 2004, 10:1507-1517. DOI: https://doi.org/10.1261/rna.5248604

20. Zaiou M, Amrani R, Rihn B, Hajri T: Dietary patterns influence target gene expression through emerging epigenetic mechanisms in nonalcoholic fatty liver disease. Biomed 2021, 9:1256. DOI: https://doi.org/10.3390/biomedicines9091256

21. van der Heijden RA, Sheedfar F, Morrison MC, Hommelberg PP, Kor D, Kloosterhuis NJ, Gruben N, et al: High-fat diet induced obesity primes inflammation in adipose tissue prior to liver in C57BL/6j mice. Aging (Albany NY) 2015, 7:256-268. DOI: https://doi.org/10.18632/aging.100738

22. Liu X, Zhao J, Liu Q, Xiong X, Zhang Z, Jiao Y, Li X, et al: MicroRNA-124 promotes hepatic triglyceride accumulation through targeting tribbles homolog 3. Sci Rep 2016, 6:37170. DOI: https://doi.org/10.1080/ 10.1038/srep37170

23. Wang JJ, Zhang YT, Tseng YJ, Zhang J: miR-222 targets ACOX1, promotes triglyceride accumulation in hepatocytes. Hepatobiliary Pancreat Dis Int 2019, 18(4): 360-365. DOI: https://doi.org/10.1016/j.hbpd.2019.05.002

24. Li DD, Liu Y, Xue L, Su DY, Pang WY: Up-regulation of microRNA-367 promotes liver steatosis through repressing TBL1 in obese mice. Eur Rev Med Pharmacol Sci 2017, 21:1598-1603. DOI: https://www.europeanreview.org/article/12530

25. Yu Y, Tian T, Tan S, Wu P, Guo Y, Li M, Huang M: MicroRNA-665-3p exacerbates nonalcoholic fatty liver disease in mice. Bioengineered 2022, 13:2927-2942. DOI: https://doi.org/10.1080/21655979.2021.2017698

26. Zhang Q, Xiao X, Zheng J, Li M, Yu M, Ping F, Wang T, et al: Vildagliptin, a dipeptidyl peptidase-4 inhibitor, attenuated endothelial dysfunction through miRNAs in diabetic rats. Arch Med Sci 2019, 17:1378-1387. DOI: https://doi.org/10.5114/aoms.2019.86609

27. Auler M, Bergmeier V, Georgieva VS, Pitzler L, Frie C, Nüchel J, Eckes B, et al: miR-127-3p Is an epigenetic activator of myofibroblast senescence situated within the microRNA-enriched Dlk1-Dio3-imprinted domain on mouse chromosome 12. J Invest Dermatol 2021, 141:1076-1086.e3. DOI: https://doi.org/0.1016/j.jid.2020.11.011

28. Chartoumpekis DV, Zaravinos A, Ziros PG, Iskrenova RP, Psyrogiannis AI, Kyriazopoulou VE, Habeos IG: Differential expression of microRNAs in adipose tissue after long-term high-fat diet-induced obesity in mice. PLoS One 2012, 7:e34872. DOI: https://doi.org/10.1371/journal.pone.0034872

29. Willekens J, Mosca P, Burt-Oberecken N, Laugeais E, Kaoma T, Bernardin F, Vallar L, et al: Cross-Talk between miRNAs from the Dlk1-Dio3 Locus and histone methylation to protect male cerebellum from methyl donor deficiency. Mol Nutr Food Res 2023, 67:e2300040. DOI: https://doi.org/0.1002/mnfr.202300040

30. Froimchuk E, Jang Y, Ge K: Histone H3 lysine 4

methyltransferase KMT2D. Gene 2017, 627:337-342.

DOI: https://doi.org/10.1016/j.gene.2017.06.056

31. Dai R, Wang Z, Ahmed SA: Epigenetic contribution and genomic imprinting Dlk1-Dio3 miRNAs in systemic lupus erythematosus. Genes (Basel). 2021, 12(5): 680.

DOI: https://doi.org/10.3390/genes12050680

32. Jin AL, Ding L, Yang WJ, Liu T, Chen W, Li T, Zhang CY, et al: Exosomal microRNAs in the DLK1-DIO3 imprinted region derived from cancer-associated fibroblasts promote progression of hepatocellular carcinoma by targeting hedgehog interacting protein. BMC Gastroenterol 2022, 22(1): 505.

DOI: https://doi.org/10.1186/s12876-022-02594-2

33. Shibayama Y, Nagano M, Hashiguchi K, Fujii A, Iseki K: Supplementation of concentrated Kurozu, a Japanese black vinegar, reduces the onset of hepatic steatosis in mice fed with a high-fat diet. Funct Foods Health Dis 2019, 9:276-296. DOI: https://doi.org/10.31989/ffhd.v9i4.596